A Two-Stage IMPATT-Diode Amplifier

HARRY A. WILLING

Abstract—**The sytem aspects and packaging of a two-stage FM IMPATT-diode amplifier are described. The amplifier combines the output power of 4 IMPATT diodes in the final stage to provide an output power of greater than 4 W at 6 GHz. The system has a locking bandwidth of greater than 200 MHz with a 16-dB gain and a noise figure of less than 50 dB. Both the design and the experimental performance of the amplifier and each of its stages are discussed. The noise characterization of IMPATT-diode amplifiers, operating as injection-locked oscillators or stable amplifiers, determined the mode of operation for each stage. Included in the paper are experimental results of large-signal noise characterization of both Si and GaAs IMPATT diodes, as are the noise characteristics related to the output power and gain.**

I. Introduction

DESIGN CRITERIA for a 6-GHz 4-W IMPATT FM power amplifier and the packaging philosophies employed in its development are discussed. System aspects are also discussed and performance results are given. The power amplifier comprises two amplifier stages. The first, or driver stage, employs dual GaAs IMPATT diodes that are power combined; the second, or output stage, employs four Si IMPATT diodes that are split into separate or dual amplifiers with power combining. The amplifier design includes the use of microstrip, stripline, and coaxial circuit techniques. The integration of these circuit techniques is discussed. This paper considers the salient features of device selection. Measured data relating to the large-signal noise performance of devices is presented and discussed. Determination of the operating mode of the IMPATT diodes—locked oscillator–amplifier or straight amplifier—was arrived at by power-noise characterization of the devices.

II. System Aspects

This FM power amplifier utilizes IMPATT diodes to obtain the desired RF power output. It was designed to develop 4 W or greater of RF power in the 6-GHz band. An overall gain of greater than 16 dB is derived from two stages of amplification. The amplifier is mechanically tunable to cover the 5.9–6.4-GHz band with an instantaneous bandwidth greater than 200 MHz.

The block diagram for the power-amplifier system is shown in Fig. 1. Fig. 2 illustrates the RF signal flow through the respective modules. The system comprises nine basic modules, four of which are employed in the direct RF signal path. Power generation in the first stage, or the driver amplifier, is developed by dual GaAs diodes. These diodes are driven and, subsequently, the output power is combined through a 3-dB 2-branch line hybrid. The diodes are mounted in separate coaxial packages which also contain the diode-matching structures. Interstage isolators are included at the input and output ports of the power-combining hybrid. The power output of the driver amplifier is hybrid split to dual output ports. The RF circuitry for the amplifier, excluding the dual coaxial structures, is contained within a common package. SMA-type connectors are used to provide the RF interconnections between the coaxial structures and the auxiliary circuitry. Either diode may be replaced without disabling the entire amplifier stage.

The second-stage amplifier comprises dual output amplifiers that are power combined. Both amplifiers are identical and each uses two high-power Si IMPATT diodes. The associated circuitry is similar to that within the driver amplifier. The dual high-power diodes are contained within a common coaxial structure; this is mechanically fastened to its microwave integrated-circuit module to form an integral module. Either of the dual output amplifiers can be removed independently from the system while maintaining system operation. The output powers of the dual power amplifiers are combined through a final hybrid combiner.

Dual power supplies—dc-to-dc converters—are used within the power-amplifier subsystem providing the necessary transformation from the −24-V dc input source to the bias voltages required by the IMPATT diodes. Each supply provides the biasing voltages to one of the dual GaAs IMPATT diodes in the driver amplifier and to both dual Si IMPATT diodes contained in one of the dual output amplifiers. The implementation of this form of biasing arrangement with dual supplies in conjunction with multiple diode operation provides the fail "soft" feature of the power amplifier. Loss of operation in the second-stage amplifier, of one, two, or three devices, will result in an output power degradation of 2.5, 6.0, or 9.0 dB, respectively. Failure of operation of all four devices will result in an output signal derived from the driver amplifier and attenuated by the path loss of the output amplifier. Loss of either or both of the dual driver amplifier diodes will result in a reduction in the system bandwidth. Catastrophic failure can occur only if a break takes place in a primary RF conductor line.

Monitoring networks and in-system test facilities are provided at key points in the subsystem. An operating failure will be translated to an output signal and a light-emitting-diode display indicating the fault location. The RF signal conditions that are monitored and translated to output signal alarms when a respective fault occurs include the input, interstage, and output power levels. Fault alarms are transmitted when the output power is degraded by 2.0 dB, or when the input and interstage power levels are degraded by 3.0 dB below their respective nominal levels. Among the conditions that are monitored are the bias voltage levels of each of the IMPATT diodes. A meter for in-system test is located on the front panel of the subsystem drawer in conjunction with a test-selector switch for selecting a given test function. Separate linear detector–amplifier circuits monitor the sampled input, interstage, and output power levels. Each of the monitored levels, as determined by the test-selector-switch position, can be displayed by the front panel meter. The front panel meter also displays the IMPATT-diode biasing currents and all auxiliary supply voltages.

Manuscript received February 21, 1973; revised May 14, 1973.

The author is with Communications and Electronics, Martin Marietta Aerospace, Orlando, Fla.

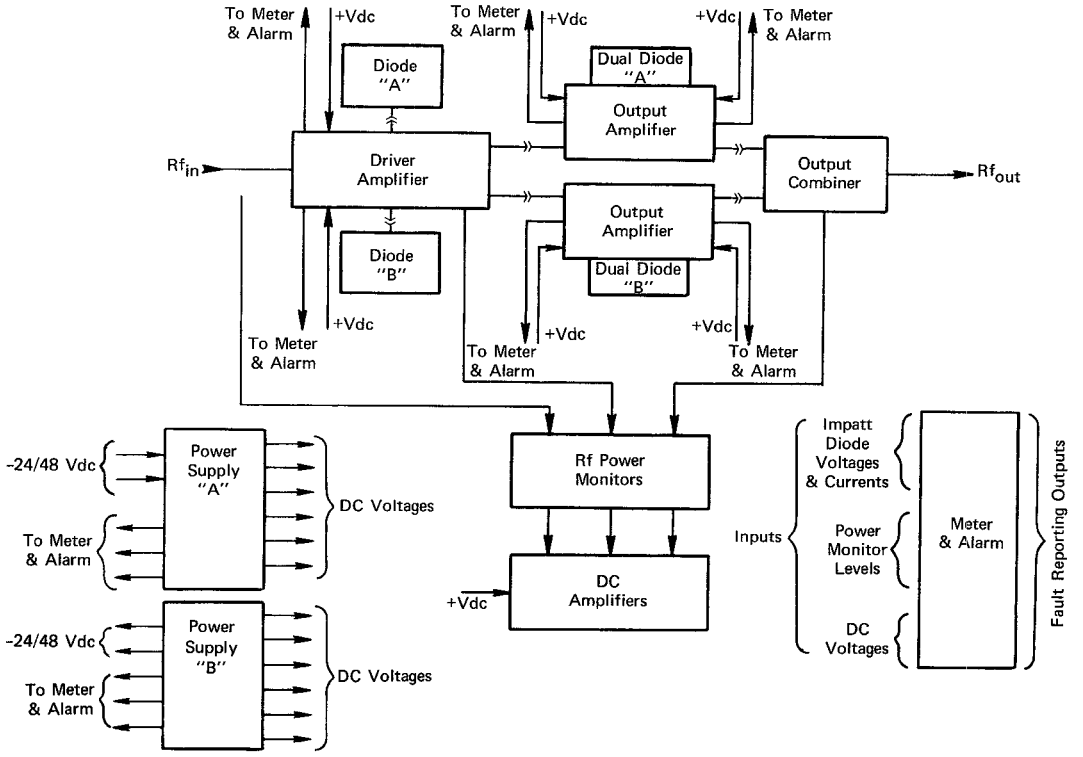

Fig. 1. Power-amplifier block diagram.

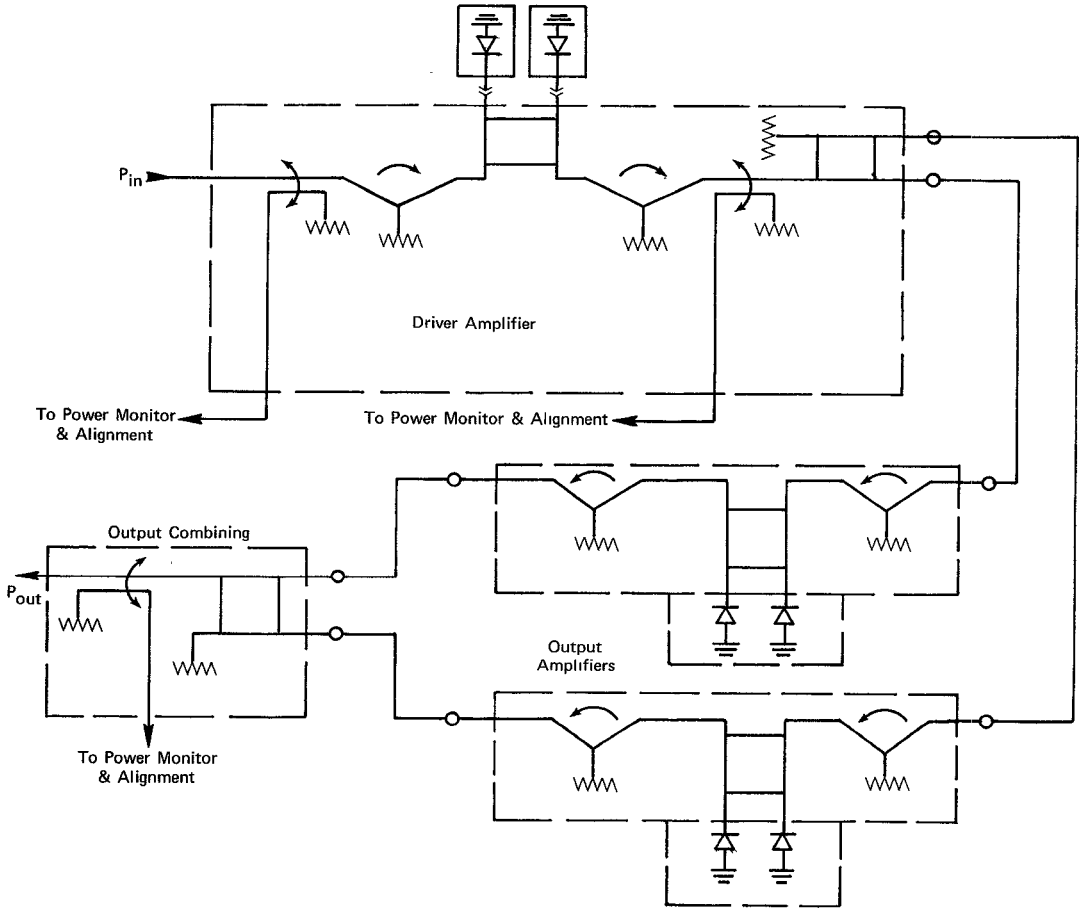

Fig. 2. Power-amplifier RF signal-flow diagram.

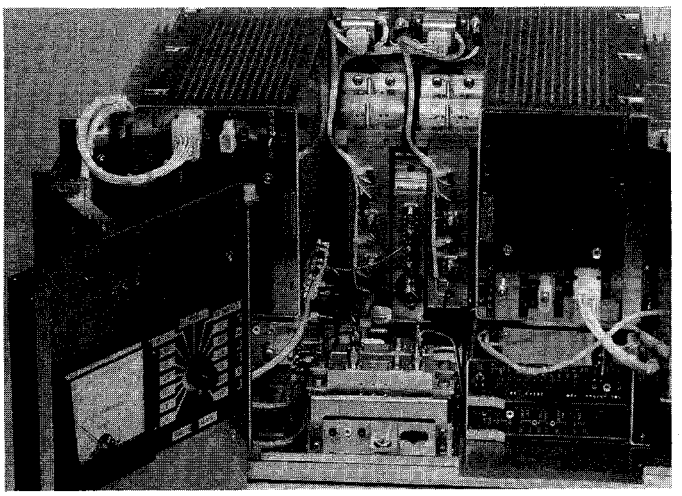

Fig. 3.

The power-amplifier subsystem, consisting of the RF modules, their dual power supplies, and the auxiliary modules, is contained in a standard $10\frac{1}{2}\times16$-in drawer for rack mounting. Fig. 3 is a photograph of the power-amplifier drawer. The backwall of the drawer and portions of the sidewalls are fabricated with integral heat fins. The coaxial structures containing the high-power devices of the output amplifiers are mounted directly against the backwall for maximum heat dissipation. The power supplies and the driver amplifier diodes are heat sinked to the sidewalls.

The 6-GHz circuitry, within the power-amplifier system, is formed by the integration of microstrip, stripline, and coaxial circuitry. The coaxial circuitry consists of the IMPATT-diode matching structures and the associated diode mounts. Simple coaxial transformers [1] are used to match the diodes, and single screw tuning within a resonant cavity located in each of the diode mounts provides a means for mechanical tuning over the 5.9–6.4-GHz band. The microstrip elements are fabricated on a 0.026-in Duroid sheet which is copper clad on one surface only; the opposite surface is bonded to an aluminum plate. The aluminum plate serves not only as the ground plane for the microstrip elements and a rigid carrier, but is also machined to serve as the bottom plate for the RF module enclosure. The 6-GHz microstrip circuitry consists of hybrids, couplers, and quarter-wave dc biasing lines; the associated discrete passive devices are bonded to their respective microstrip elements. The circulators are fabricated using both microstrip and stripline techniques. The RF ports of the circulator resonator are bonded directly to their associated microstrip impedance-matching elements. The techniques that are employed in the integration of the microstrip and stripline elements assure continuous ground plane integrity.

The dc biasing, developed from the dual -24-V dc-to-dc converters, is applied to each of the IMPATT diodes through series resistors that are integrated with each of the amplifier modules. To minimize the low-frequency baseband noise characteristics, 50-Ω carbon resistors were used with each of the Si diodes in the output amplifier and each of the GaAs diodes employed 100-Ω resistors [2].

III. System Performance

The system specifications for the power amplifier included an input-drive power level of $+18$ dBm and an overall amplifier gain of greater than 18 dB. The resultant output power level was required to be 4 W or greater. Device characterization indicated that the amplifier would meet these goals, yet provide the best noise performance if it were designed as a single-stage injection-locked oscillator. However, to obtain the high gain, an output power level within a single-stage injection-locked oscillator would result in a narrow locking bandwidth. System distortion requirements established a third order or parabolic delay distortion of less than -13 dBrncO (84.6 dB, NPR) and a second order or slope delay distortion of less than -5.5 dBrncO (77 dB, NPR). The expressions for the second- and third-order distortion for injection-locked oscillators have been developed by Ramadan [3]. The second-order distortion to signal-ratio (NPR) expression is

$$D_{2/S} = 10 \log \left[\frac{16 f^2 \Delta f_0^2}{B_L^6} \sigma^2 (2 - f/f_b) \right], \quad f \leq 2f_b. \tag{1}$$

The third-order NPR expression is

$$D_{3/S} = 10 \log \left[\frac{8}{3} \frac{f^2 \sigma^4}{B_L^6} (3 - f^2/f_b^2) \right], \quad f \leq f_b \tag{2}$$

where

f modulation frequency (MHz);
f_b top baseband frequency (MHz);
B_L total locking bandwidth (MHz);
σ composite rms frequency deviation (MHz);
Δf_0 frequency difference between the locking signal and the free-running oscillator.

A frequency difference Δf_0 between the locking signal and the free-running oscillator of 35 MHz was permitted to provide for temperature variation, long-term device parameter change, and factory alignment. To obtain a second-order distortion to signal ratio of less than 77 dB in an 1800-channel system with an allowed frequency difference of 35 MHz required a system locking bandwidth of 200 MHz or greater. Consequently, it was necessary to design the power amplifier as a two-stage amplifier. Both stages were designed to provide approximately 9–10 dB of midband gain at the device ports. The first stage, or driver amplifier, was designed to operate as an injection-locked "soft" oscillator. The subsystem locking bandwidth of the driver stage only is greater than 500 MHz. The dual output amplifiers, comprising the second stage, were also designed as injection-locked "soft" oscillators with a locking bandwidth of 225 MHz, which defines the system bandwidth. Further considerations in the design of the system amplifiers and device selection are discussed in Section IV. Also included in Section IV are amplifier and device performance curves.

The output power responses of the power amplifier, under the conditions of full operation and, subsequently, at output levels equivalent to single- and multiple-output device failures, are plotted in Fig. 4. The horizontal grid lines appearing on the graph indicate the predicted power degradation, attributed to successive output device failure. Curve 5 is the output power response after complete failure of each device in the output amplifier. This response curve is an output power plot of only the driver amplifier operating through the system. The much wider operating band of the driver amplifier only can be seen.

The locking bandwidth, output power, and noise figure of the power amplifier, measured with respect to the input-drive power, are plotted in Fig. 5. The wide locking band-

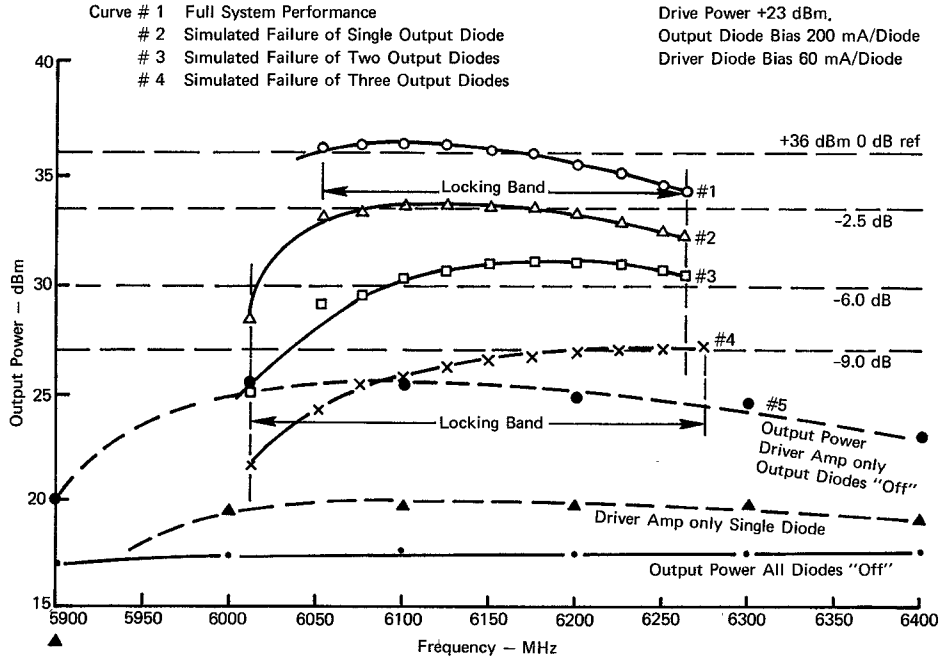

Fig. 4. Power-amplifier subsystem power-response curves.

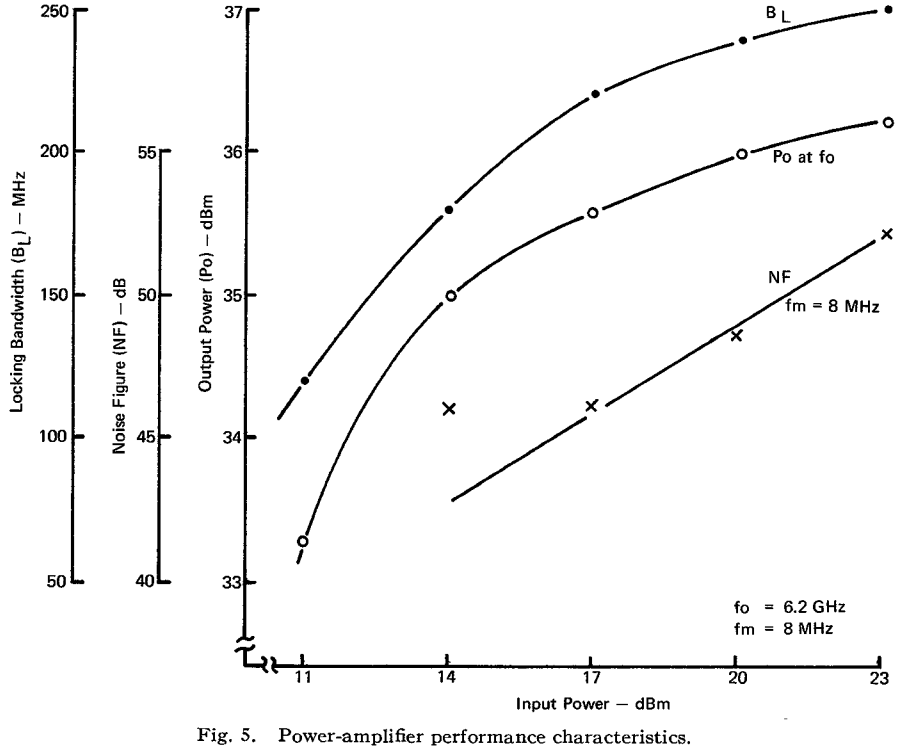

Fig. 5. Power-amplifier performance characteristics.

widths and the increase in output power with increasing driver power indicate the degree of "softness" of the driver and output-stage injection-locked oscillator–amplifiers. The noise figure as measured at 8 MHz from the carrier is a direct function of the input power. This phenomenon was of paramount consideration in device selection and is discussed in Section IV.

The AM–PM conversion of the power amplifier was determined by the two-tone signal method. At the +18-dBm input-signal level, the AM–PM conversion was determined to be 7.4°/dB [4].

IV. Device Considerations and Module Design

The overall system design established an input level of +18 dBm to the power-amplifier system with a required gain of 18 dB to develop a minimum output power level of +36 dBm. A maximum 50-dB noise figure was assigned to the power amplifier; however, the goal was to develop the output

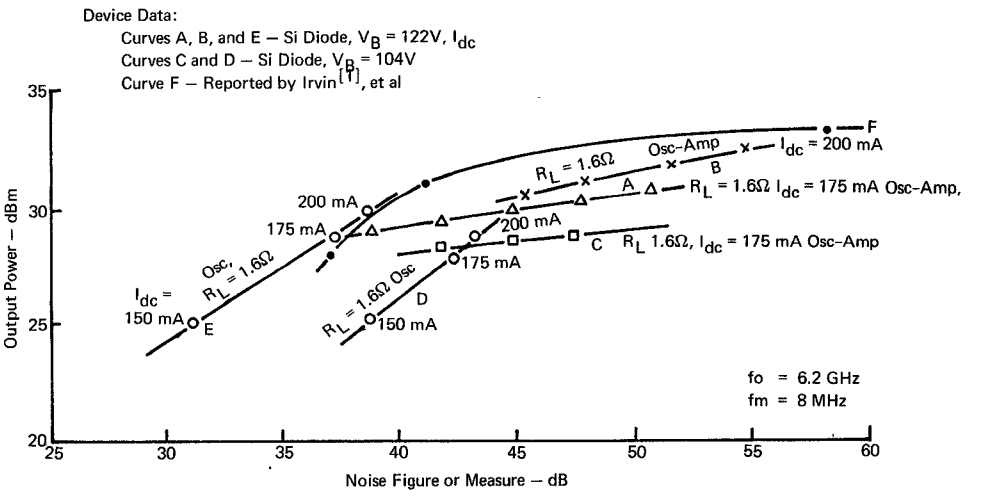

Fig. 6. Output power–noise characteristics of Si IMPATT-diode amplifier–oscillators.

power level with a minimal noise figure. The realization of the gain and power output requirements was attained through two stages: a driver and an output amplifier stage.

The selection of the IMPATT diodes in the driver and output amplifier stages and the establishment of their mode of operation were based upon measurements of the interdependence of power output and noise performance. The diodes were characterized in coaxial test fixtures equivalent to the structures used in the amplifier modules. Their mode of operation, as amplifiers or as locked oscillator–amplifiers, was changed by altering the impedance-matching transformer in the coaxial fixture. Under the differing operating conditions, measurements were made to establish the power output and noise-performance characteristics of the devices.

The output amplifier design utilized four 1.5-W Si IMPATT diodes to establish the system output requirement of 4.0 W at 6.0 GHz. To determine the power-noise characteristics of the devices, Si diodes having breakdown voltages of 107 V dc and 122 V dc were tested. The junction areas of the devices are 6.5×10^{-4} cm^2 and 8×10^{-4} cm^2, respectively. Each device type was operated in the free-running oscillator mode and as an amplifier or injection-locked oscillator–amplifier, and their performance characteristics were measured. In the free-running oscillator mode, the noise measure was determined from experimental data taken for both devices using the relationship [1]

$$\Delta f \text{ rms} = f_0/Q_{\text{ext}}\left(\frac{kT_0MB}{P_0}\right)^{1/2} \tag{3}$$

where

Δf rms	rms noise deviation at modulation frequency f in a narrow window of width B;
f_0	oscillator frequency;
Q_{ext}	external circuit Q;
M	large-signal noise measure;
B	measurement bandwidth;
P_0	oscillator power output.

In the amplifier or locked oscillator–amplifier mode, the noise figure was determined from the relationship (see the note, as follows)

$$\Delta f \text{ rms} = (kT_0N_fB/C)^{1/2}f \tag{4}$$

in addition to the terms previously defined:

C	input carrier power (watts);
f	frequency in modulation spectrum (hertz).

Note: This is as derived from the expression (see [5])

$$(S/N_0) = (C/N_i)(B/B_C)(\Delta F_m/\bar{f}_n)^2$$

where

$\bar{f}_n$	$=f$—frequency in modulation spectrum;
ΔF_m	$=\sqrt{2}\,\Delta F_{m_{\text{rms}}}$;
B	IF bandwidth;
B_C	channel bandwidth or measurement bandwidth;
N_i	$=2kTBN_f$;
S_0	$=(\Delta F_m/\sqrt{2})^2$;
N_0	$=(\Delta f \text{ rms})^2$.

Therefore,

$$1/(\Delta f \text{ rms}^2) = C/(kTN_f)(1/B_C)(1/f)^2$$

or

$$\Delta f \text{ rms} = [(kTN_fB_C)/C]^{1/2}f.$$

Fig. 6 illustrates the noise figure as a function of output power for the Si devices operating under differing conditions. The measured characteristics shown plotted in curves A, B, and E were taken of an Si diode having a breakdown voltage of 122 V and a junction capacitance at breakdown of approximately 1.0 pF. The same diode load resistance was employed in plots A and E. In plot E the diode was operated in the free-running oscillator mode and the output power was varied by adjusting the dc biasing current to 150, 175, and 200 mA. The oscillator was subsequently operated at the 175-mA level and phase locked at increasing injected signal levels. The measured output power versus noise-figure characteristics are shown in plot A. The measurements shown in plot B were obtained from a wider band lower gain oscillator–amplifier operating at a current of 200 mA.

Employing a diode with a reduced breakdown voltage (104 V dc), with an equivalent junction capacitance at breakdown, resulted in degraded output power–noise-figure characteristics. The results are plotted in curve D for the free-running oscillator mode, and in C for the locked oscillator–

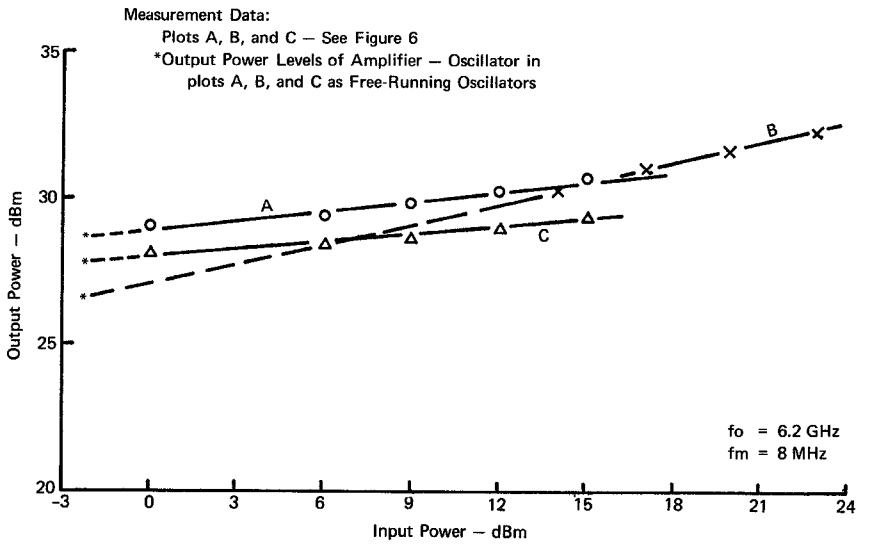

Fig. 7. Power-response characteristics of IMPATT amplifier–oscillator.

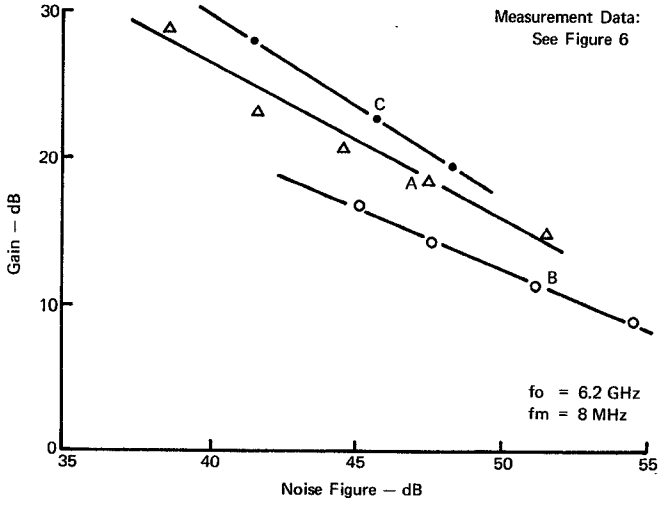

Fig. 8. Gain–noise characteristics of Si IMPATT amplifier–oscillators.

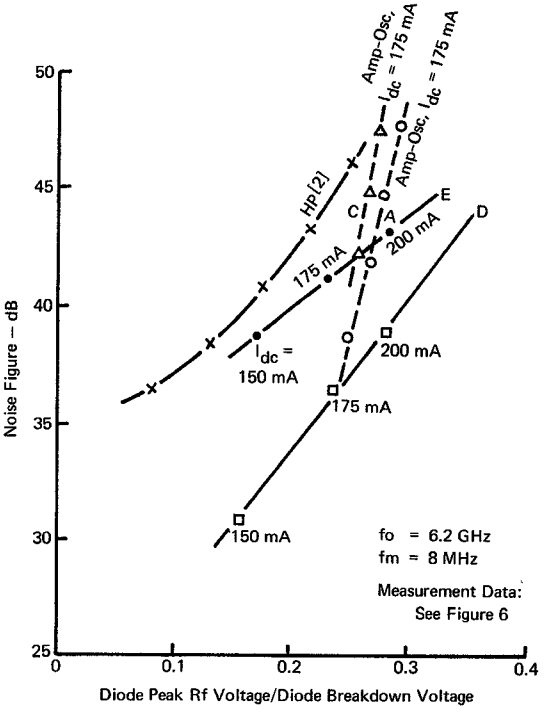

Fig. 9. Noise characteristics of Si IMPATT diodes as a function of the ratio of peak RF voltage to breakdown voltage.

amplifier mode. Included in these sets of curves is the power–noise-figure characteristic of an IMPATT oscillator (curve *F*), employing an Si diode with a breakdown voltage of 125 V, as given by Irvin *et al.* [4]; a close agreement exists between the reported data.

The input–output power response curves of the oscillator–amplifiers characterized in Fig. 6 are shown in Fig. 7. Their gain–noise characteristics are illustrated in Fig. 8. It can be noted in Fig. 7 that the oscillator–amplifier, whose response is shown in plot *B*, exhibited the greatest change in its input–output power response. It is operated more as a "soft" oscillator or straight amplifier, i.e., with the lowest external Q, Q_{ext}, and, consequently, the widest locking bandwidth and reduced gain. It can be noted from these sets of curves that at a fixed biasing condition and at large-signal conditions, over a fairly wide range of input power, the amplifier will add a constant amount of FM noise; however, at higher input power levels, the signal intermodulation distortion is decreasing [see (1) and (2)]. Hence, a wider operating band at a reduced gain is realized at the expense of a degraded noise figure [see (4)].

Known values of the output loading across the diode terminals permitted the determination of the diode's peak RF voltage in operating modes and power output levels indicated in Figs. 6–8. The ratio of the calculated peak RF voltage to the diode breakdown voltage is plotted against the respective levels of noise measure or noise figure in Fig. 9. Included for comparison in this figure are curves published by Hewlett-Packard [1].

Based upon anticipated improvement in their output power–noise-figure characteristics, GaAs IMPATT diodes were

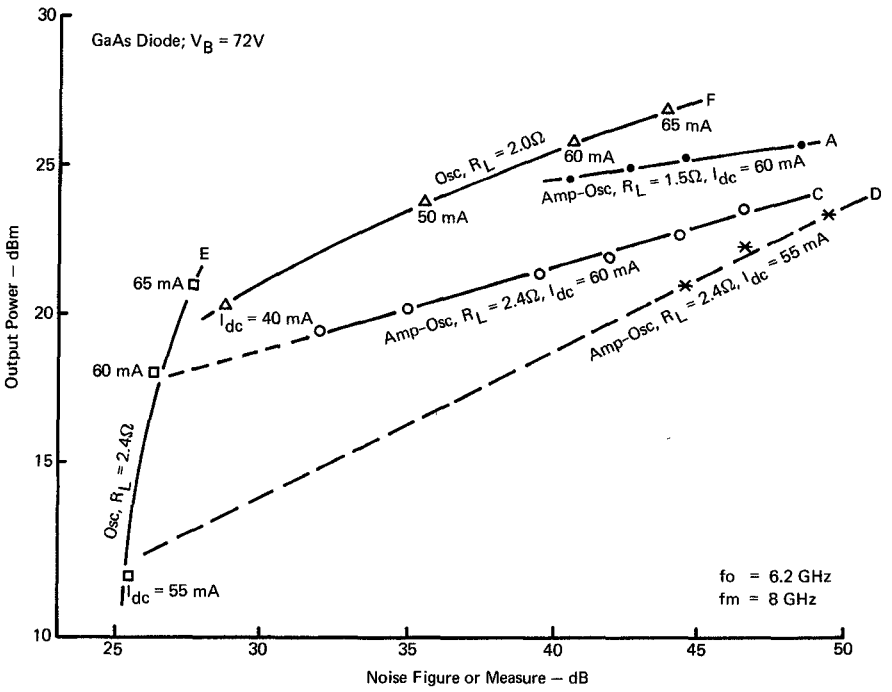

Fig. 10. Output power–noise characteristics of GaAs IMPATT-diode amplifier–oscillator.

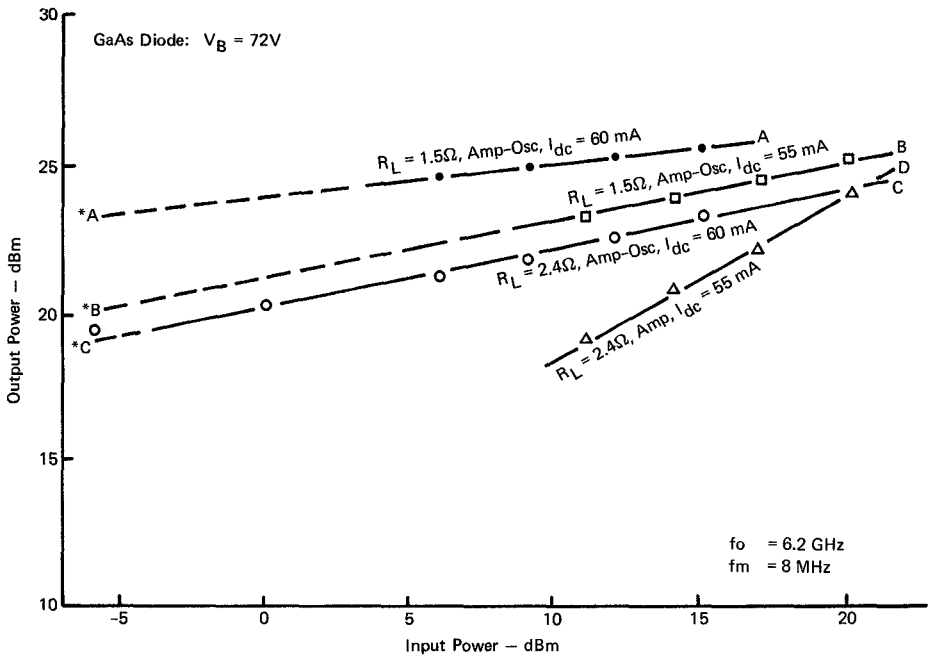

Fig. 11. Power-response characteristics of GaAs IMPATT amplifier–oscillators.

chosen to be employed in the driver amplifier. The diodes selected were rated as 0.5-W devices operating at a nominal current of 80 mA with a typical breakdown voltage of 72 V. Tests were conducted to determine the power–noise characteristics of these devices. The measurements were similar to those taken for the 1.5-W Si devices, and the results are plotted in Figs. 10–13.

The series of plots in Fig. 10 are measured data taken with the GaAs device operating in the free-running oscillator mode and the locked oscillator–amplifier mode. In the free-running oscillator mode, output power–noise characteristics were taken at the specified steps in the dc biasing current for load values of 2.4 and 2.0 Ω, and are illustrated in curves *E* and *F*. In the locked oscillator–amplifier mode, the output power was increased by increasing the level of the injected or locking signal. The measured output power–noise-figure characteristics are plotted for differing load lines and biasing currents (curves *A*, *B*, *C*, and *D*).

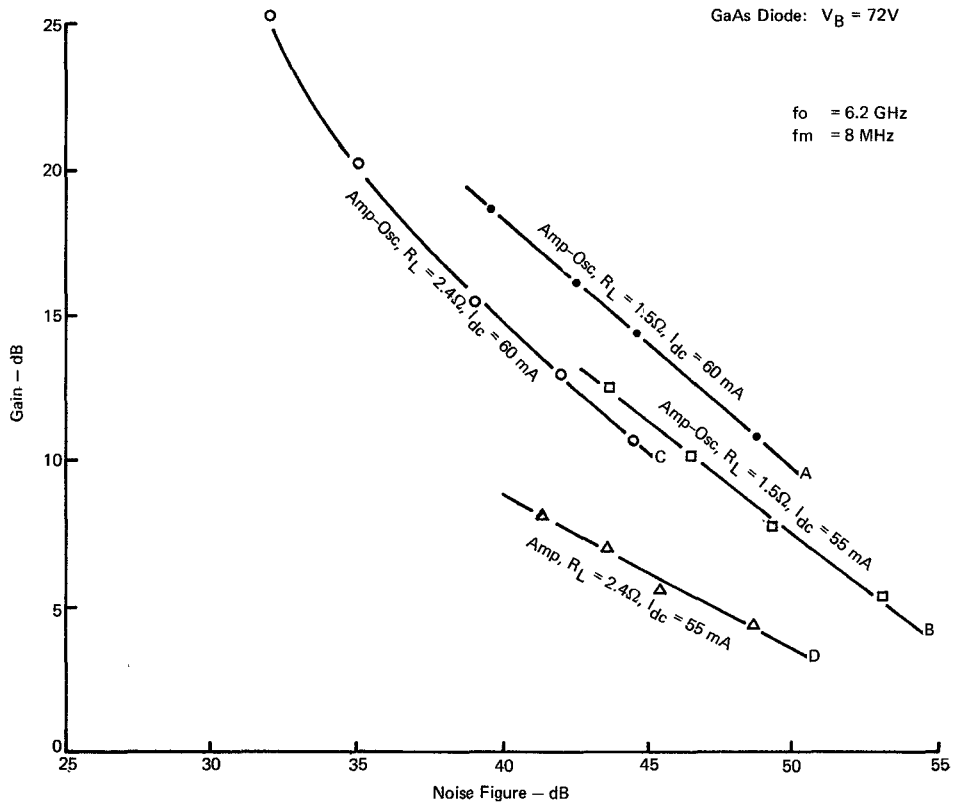

Fig. 12. Gain–noise characteristics of GaAs IMPATT amplifiers.

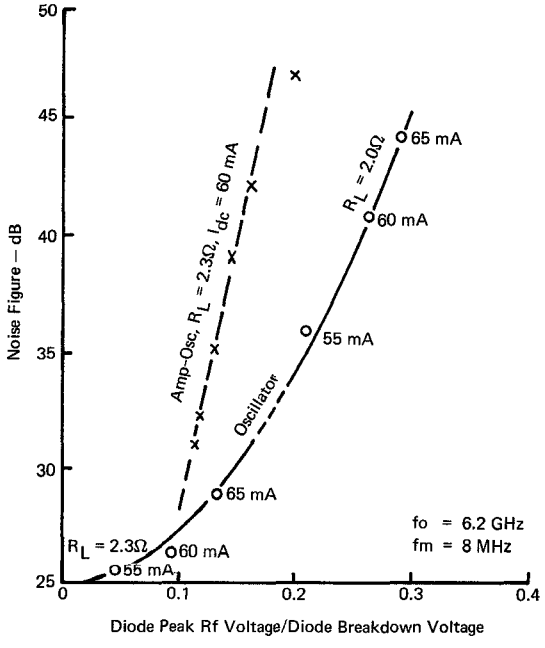

Fig. 13. Noise characteristics of GaAs IMPATT diodes as a function of the ratio of peak RF voltage to breakdown voltage.

Analogous to the Si-device characteristics, the degradation in the noise-figure performance of the GaAs device from the free-running oscillator mode to the locked oscillator–amplifier mode can be noted. The poorest output power–noise-figure performance is illustrated by plot D of Fig. 10. This plot was derived from data obtained from a locked oscillator–amplifier that exhibited the greatest change in output power versus input power and the widest locking bandwidth or lowest Q_{ext}. That is, it performed as the "softest" oscillator. Conversely, it can be seen that the best noise performance can be obtained for a given output power level by designing a high-gain narrow locking band oscillator–amplifier. It is also to be noted that output power–noise-figure characteristics of the amplifier are degraded if the injected power is increased to compensate for a reduction in the biasing current.

Figs. 11 and 12 show the input–output characteristics and the gain–noise-figure characteristics of the oscillator–amplifiers plotted in Fig. 10. From the oscillator data derived and plotted in curves E and F of Fig. 10, the ratios of the peak RF voltages to the diode breakdown voltages were determined. A plot of the voltage ratios to their respective noise measures or figures is shown in Fig. 13 Comparing the GaAs noise-performance plot in Fig. 13 to the Si noise-performance plot in Fig. 9, improved GaAs versus Si IMPATT-device noise-figure performance is achieved for diode peak RF voltage to breakdown voltage ratios of less than approximately 0.1; above this ratio, comparable performance was obtained.

Each of the dual output amplifiers was designed as an injection-locked oscillator to provide the best noise performance. They operated with a locking bandwidth of greater than 200 MHz and provided a power output of greater than +33.5 dBm at an input drive level of +23 dBm. The matching loads to each of the dual diodes is 1.6 Ω, and the biasing current operating each of the Si IMPATT devices is 200 mA. The biasing current was established by restricting the device junction temperature rise to less than 165°C, where the

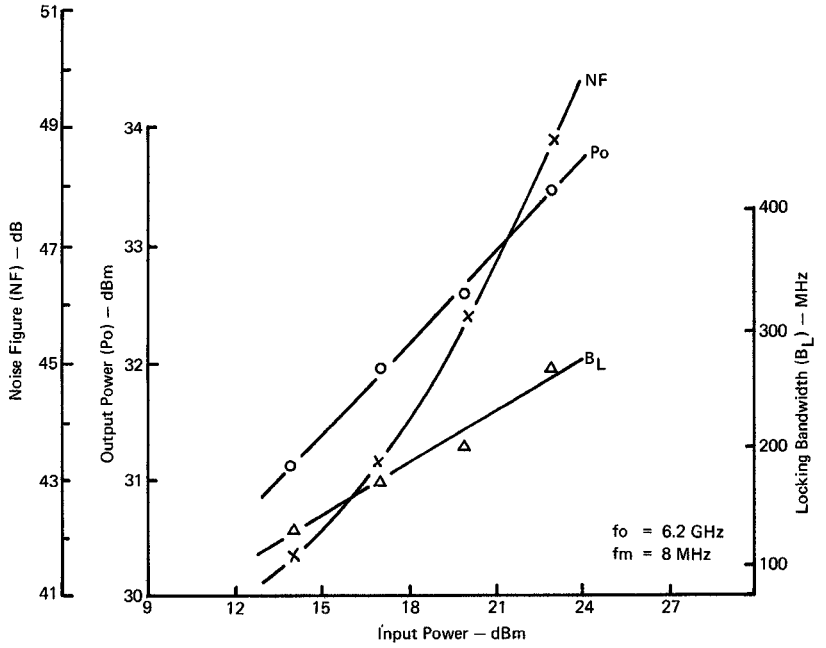

Fig. 14. Si (dual diode) IMPATT-amplifier performance.

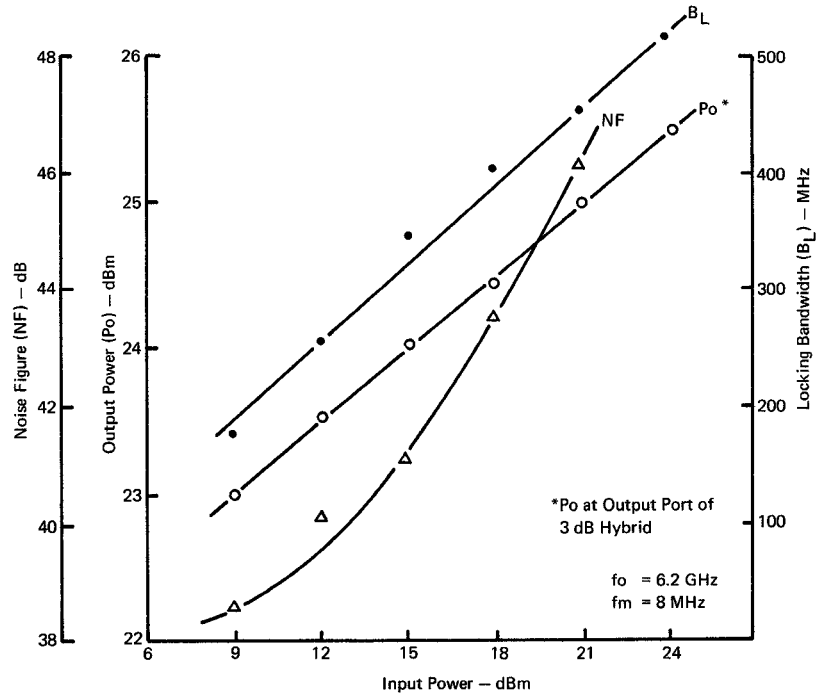

Fig. 15. GaAs (dual diode) IMPATT-amplifier performance.

maximum thermal resistance was specified to be 6° C/W or less. From Figs. 6 and 7, plot *B*, it is seen that at this drive level the output power should be +31.5 dBm per device and a noise figure of 49 dB should be obtained. The actual measured performance of the output amplifier is shown in Fig. 14. At the +23-dBm input level, an output power level of +33.9 dBm, a noise figure of 48.7 dB, and a locking bandwidth of 270 MHz are obtained.

The driver amplifier design provided the input power-level requirements at the output amplifiers. The amplifier is designed to have a gain of greater than 9.0 dB, at an input level of +18 dBm (i.e., approximately +14.0 dBm to each of the dual diodes). The diode's load resistor is 2.4 Ω and the biasing current is 65 mA. Referring to Figs. 10 and 12, plots *C*, a noise figure of less than 45.0 dB can be expected at a 9.0-dB-gain +18-dBm input level. The driver amplifier performance is plotted in Fig. 15. As shown, at the +18-dBm input level, the output power at each of the output hybrid ports is greater than +24.0 dBm, while the locking bandwidth is 400 MHz and the noise figure is 43.5 dB.

Based upon the driver stage gain of 9 dB and the respective noise figures of both stages, the composite noise figure of the two-stage amplifier is calculated to be 45 dB. The measured noise figure for the two-stage amplifier as plotted in Fig. 5 projects a noise figure of +47 dB at an input drive level of +18 dBm.

V. Conclusions

A strong interdependence exists between the output power, gain, and noise figure of IMPATT amplifiers or injection-locked oscillators (oscillator–amplifiers). An IMPATT-diode oscillator–amplifier exhibits the most desirable output power–noise-figure relationship when the device is operated under minimum injected signal levels. The noise figure of an IMPATT oscillator–amplifier, designed to provide a specified output power level under a given biasing condition, is minimized when the device is matched to provide this output in the free-running mode. It is operated as a high-gain narrow locking band amplifier–oscillator. Increasing the RF load resistance at the diode will reduce the free-running output level and improve the small-signal noise figure. However, this oscillator–amplifier, with lower gain and wider band features under the drive conditions necessary to reestablish the output power of the high-gain oscillator–amplifier, will exhibit a degraded noise figure.

Acknowledgment

The author wishes to thank D. E. Wunsch and D. Bowyer for their technical assistance, and J. Norton for his careful measurements; all are Communications and Electronics employees at the Orlando Division of Martin Marietta Aerospace.

References

[1] "Microwave power generation and amplification using Impatt diodes," Hewlett-Packard Components, Application Note 935.
[2] C. A. Brackett, "The elimination of tuning-induced burnout and bias circuit oscillators in Impatt oscillators," *Bell Syst. Tech. J.*, vol. 52, pp. 271–306, Mar. 1973.
[3] M. Ramadan, "Intermodulation distortion of FDM-FM in injection-locked oscillator," *IEEE Trans. Commun.*, vol. COM-21, pp. 191–194, Mar. 1973.
[4] L. P. Laico, H. L. McDowell, and C. R. Moster, "Traveling wave tube for 6000-Mc radio relay," *Bell Syst. Tech. J.*, pp. 1285–1346, Nov. 1956.
[5] P. F. Panter, *Modulation, Noise, and Spectral Analysis*. New York: McGraw-Hill, 1965, p. 442.

IMPATT-Diode Power Amplifiers for Digital Communication Systems

S. F. PAIK, P. J. TANZI, AND DOUGLAS J. KELLEY

***Abstract*—IMPATT-diode amplifiers with a power output of 1.0 W have been developed for use in an 11-GHz digital radio. Two types of amplifiers, a multistage reflection amplifier and a hybrid amplifier containing an injection-locked oscillator stage, have been evaluated by measuring the bit error rate degradation due to the amplifier. System test data show that the stable amplifier introduces little or no errors while the injection-locked oscillator (ILO) often introduces an error-rate floor.**

I. Introduction

IMPATT-diode amplifiers with power outputs of 1 W or more have been found useful as power amplifiers in microwave communications systems. As the need for high-speed data transmission rises, it is important to establish the capability of the new type of amplifiers to transmit digitally modulated microwave carriers. The purpose of this paper is to present experimental results describing transmission characteristics of IMPATT-diode amplifiers designed for use in an 11-GHz digital radio equipment. The equipment is designed to transmit quadrature phase-shift-keyed (QPSK) [1] carrier modulated at the data rate of 40 Mbit/s.

Two different types of IMPATT-diode amplifiers have been tested for this system: a multistage reflection amplifier [2]–[4] and a hybrid amplifier containing an injection-locked oscillator (ILO) stage [5]–[8]. Both types of amplifiers have a gain of 30 dB at the output power level of 1.0 W. Design considerations and the performance characteristics of the two types of amplifiers are described in Section II.

The most meaningful indicator of the system performance in data transmission is the bit error rate (BER). To assess the "quality" of the amplifiers, the BER degradation introduced by the amplifiers is measured by comparing the system BER with and without the amplifiers in the transmission path. In Section III the experimental results are presented, with a short description of the equipment and test conditions.

II. Amplifiers

The power output requirement for the amplifier is 1.0 W. The input signal to the amplifier is derived from an up-converter whose output level is in the range of 1–2 mW [9], and thus the minimum gain of the amplifier at the saturated output level of 1.0 W is 30 dB. Since the spectral width of the

Manuscript received February 14, 1973; revised April 30, 1973.
S. F. Paik and D. J. Kelley are with the Special Microwave Devices Operation, Raytheon Company, Waltham, Mass. 02154.
P. J. Tanzi is with the Communication Systems Laboratory, Raytheon Company, Norwood, Mass. 02062.